Numerical Simulation of High Temperature PEM Fuel Cell Performance under Different Key Operating and Design Parameters

Ahmed Mohmed Dafalla[1,2,3], Jinxiang Liu[2,*], Nana Wang[2], A.S. Abdalla[2] and Fangming Jiang[1,*]

[1]*Laboratory of Advanced Energy Systems, CAS Key Laboratory of Renewable Energy, Guangdong Key Laboratory of New and Renewable Energy Research and Development, Guangzhou Institute of Energy Conversion, Chinese Academy of Sciences (CAS), China*

[2]*School of Mechanical Engineering, Beijing Institute of Technology, Beijing 100081, China*

[3]*University of Chinese Academy of Sciences, China*

Abstract: The negative environmental impacts of internal combustion engines have changed the interest of scientists towards fuel cell engines. Using Proton Exchange Membrane (PEM) fuel cell operating under higher temperature solves some of the well-known low temperature problems. In this study, a numerical simulation has been carried out using a three-dimensional model in COMSOL to evaluate the performance of high temperature PEM (HT-PEM) fuel cell under different conditions. The obtained polarization curve for selected voltage was compared with published experimental data, and it shows a good agreement. The simulation results in terms of reactants (hydrogen and oxygen) concentrations and water production on the anode and cathode sides is presented. The influences of some key parameters on HT-PEM fuel cell performance were investigated. It was found that as the temperature and pressure increase, the performance of the HT-PEM fuel cell improves. The enhanced reaction rate and a better supply of reactants were observed to have a positive influence on HT-PEM fuel cell performance. Additionally, the results show that considering a higher permeation rate on the gas diffusion layer can enhance the performance of the fuel cell. This work provides a guideline to design and optimize a HT-PEM fuel cell with a better capability.

Keywords: HT-PEM fuel cell, Modeling, Computational Fluid Dynamics, Electrode porosity, Permeation rate.

1. INTRODUCTION

Polymer Electrolyte Membrane (PEM) fuel cell is one of the promising and most efficient power sources nowadays, particularly for vehicle applications. Vehicle engines that depend on fossil fuels are the main cause of pollutant emissions and fossil fuel consumption [1]. Therefore, to battle global warming and fluctuating oil prices, the technology of hybrid engines was developed. Although hybrid vehicles have less fuel consumption and less production of pollutants, they still have the problem of depending on finite and harmful sources of energy. In 30 years, the world's fossil fuel supplies will begin to diminish and most of the countries will need to change the energy infrastructure [2]. Changing this infrastructure will be quite costly, but it is a necessary step. Research is now mainly focused on the fuel cell system to be used in the future instead of internal combustion engines [3]. The advantages of fuel cells are quite numerous; they have a greater efficiency compared to internal combustion engines [4]. In addition, this system has virtually no harmful emissions, which makes it an excellent power source for next generation vehicles. The efficiency of energy conversion on fuel cells is much higher than that of a power station which runs on coal or a conventional car engine [5].

Recently, high temperature PEM fuel cells have received more attention for various applications mainly due to their simplified water management, improved mass transfer, and enhanced tolerance for CO poisoning [6,7]. The fuel cell stack operates in a range of temperature between 120 to 200^{o}C [8]. Under this high operating temperature, the water will only exist as vapor water and hence avoid the problems associated to flooding phenomena, which occurs in low temperature PEM fuel cells [9]. In addition, as it is able to mitigate CO poisoning, that could give a plenty of fuel options in the future instead of only using pure hydrogen in fuel cell applications [10].

Several experimental and numerical studies have been performed to investigate the heat, mass, and charge transport phenomena in HT-PEM fuel cells [11–15]. Most of the published papers focused on developing the materials of different layers to achieve the target goals for various applications under different operating conditions [16-19]. Cheddie *et al*. [20,21] provided various numerical models considering a number of different operating conditions, membrane and catalyst layer properties. Siegel *et al*. [22] presented a wide range of HT-PEM fuel cell numerical models, mainly addressing the fluid, the solid-phase temperatures and the PBI/H_3PO_4 sol-gel membrane

*Address correspondence to these authors at the Laboratory of Advanced Energy Systems, CAS Key Laboratory of Renewable Energy, Guangdong Key Laboratory of New and Renewable Energy Research and Development, Guangzhou Institute of Energy Conversion, Chinese Academy of Sciences (CAS), China; Tel: +86 20 87057656, Email to: fm_jiang2000@yahoo.com
School of Mechanical Engineering, Beijing Institute of Technology, Beijing 100081, China; Tel: +86 10 6891 1392, E-mail: liujx@bit.edu.cn

E-ISSN: 2409-5826/19

behavior. Along with this, a complete HT-PEM fuel cell model was proposed by them in [23], their model predictions were experimentally validated and compared to the measurements of real operating conditions, correspondingly Arrhenius approach was created to be used within a selected range of temperatures and it may predict the PBI/H_3PO_4 sol-gel membrane conductivity when a higher solid-phase temperature was introduced. Ubong *et al*. [24] proposed a single channel three-dimensional model with infinitely thin catalyst layer in which an agglomerate approach was used to create the electrochemical reactions, where reaction layer kinetics were highlighted. A simplified two-dimensional model was presented by Shamardina *et al*. [25] to investigate the crossover effect. Furthermore, Sousa *et al*. [9] employed a two-dimensional model to investigate how the reaction layer properties influence the cell performance. Peng *et al*. [26] proposed both steady state and transient models for HT-PEM fuel cell to demonstrate that the thermal management is a significant factor on the fuel cell performance, and discussed key optimization parameters to improve the performance. Reddy *et al*. [27] presented a parametric study that included a usage of an external coolant system of a HT-PEM fuel cell and the study focused on the temperature variations within the stack, the number of coolant plates, and the coolant flow. A three-dimensional model of HT-PEM fuel cell with a 200 cm^2 and five-cell short stack was provided by Kvesic *et al*. [28]. Their model was formed in the shape of a multi-domain, multi-scale model that gave a chance for an entire stack simulation with relatively less computational power and simulating time. Also, segmented measurements of temperature and current density were compared to the simulation results. Luke *et al*. [29] investigated the HT-PEM fuel cell stack performance and they claimed that oxygen reduction will cause the uneven current density distribution. Additionally, they explained that it is possible to achieve homogenization without reducing the stack voltage if the fuel cell works with reformat when switching from co-flow to counter-flow configuration.

In another study, Sousa *et al*. [30] presented a non-isothermal model of a HT-PEM fuel cell, by treating the catalyst layers with a spherical catalyst particle agglomerates having a porous inter agglomerate space. They also studied the effects of different geometries on the performance, and they found that along-the-channel, the model did not characterize the overall performance trend, approving that particular modeling geometry is not fit for fuel cell simulations. Jiao *et al*. [31] studied the effect of the contamination such as the carbon monoxide poisoning in HT-PEM fuel cells with various flow channel geometries. In addition, issues such as cost reduction and durability are still challenging points for HT-PEM fuel cell commercialization. Therefore, the HT-PEM fuel cells durability [32], life time [33], and degradation [34] have been highlighted and researched. Reimer *et al*. [35] used a one dimensional empirical model to explore the degradation behavior of the HT-PEM fuel cell.

The HT-PEM fuel cell has various operating and design conditions. However, the studies of parametrical effects on the performance of HT-PEM are limited [10] , and there is a need for further insight for the internal behavior of the HT-PEM fuel cell. In this paper, the effects of different key operation and design parameters are explored, displayed and discussed. A 3-D model is presented and employed for this study and further validated by pervious experimental results. This work helps to provide insight for the internal behavior of HT-PEM fuel cell.

2. HT-PEM FUEL CELL MODEL

2.1. Model Description

A single channel HT-PEM fuel cell is considered. Figure **1** shows a three-dimensional geometry model which consists of the membrane, flow channels, GDLs, catalyst layers, and current collectors on both electrodes' sides. Oxygen (O_2) and hydrogen (H_2) are supplied through gas channels in the cathode and anode sides, respectively. Then the supplied gases diffuse through the gas diffusion layers to the catalyst layers where the reactions take place. The generated protons at the anode CL are transported to the cathode side, while the electrons are transferred to the external electrical circuit via the anode and cathode current collectors. The geometrical parameters of the model are summarized in Table **1**. Table **2** describes the physical parameters used in the numerical model.

2.2. Model Assumptions

This model has the following assumptions:

- Steady-state operating conditions.
- Water exists only as vapor phase.
- Laminar flow is assumed inside the channels.
- All gases are treated as ideal gases.
- The membrane is assumed to be completely impermeable to gases.
- The materials of the components of the cell are considered isotropic and homogenous.
- There is no heat transfer towards the surroundings.

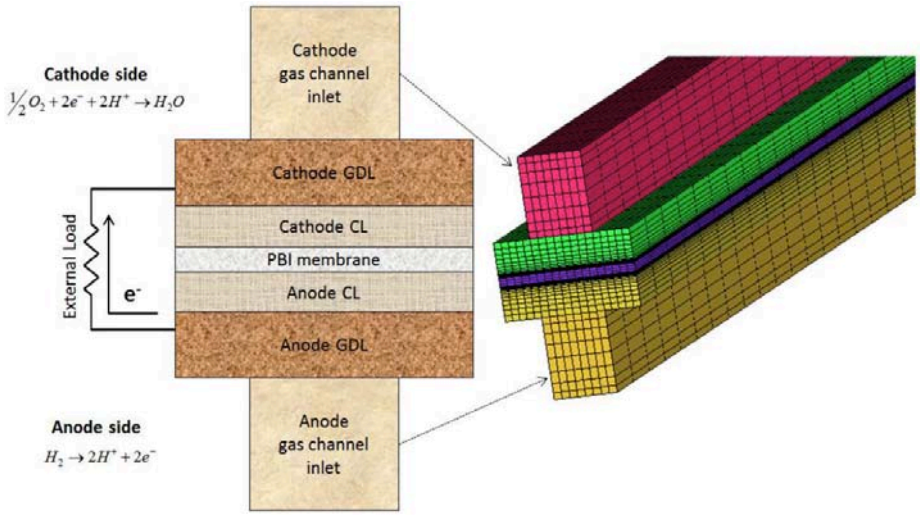

Figure 1: Computation domain and mesh of HT-PEM cell with a single channel.

Table 1: Geometrical Parameters

Description	Value (mm)
Cell length, width	20, 1.68
Channel height	1
Rib width	0.9
Channel width	0.78
GDL height	0.38
Porous electrode height	0.05
Membrane height	0.1

Table 2:

Description	Value	Unit
Porosity of GDL/CL	0.4/0.3	-
Permeability of GDL/CL	$1.18\cdot10^{-12}/2.36\cdot10^{-13}$	m^2
GDL electric conductivity	222	S/m[9]
Membrane ionic conductivity	9.825	S/m[10]
Inlet H_2 mass fraction (anode)	0.743	-
Inlet H_2O mass fraction (cathode)	0.023	-
Anode inlet flow velocity	0.2	m/s
Cathode inlet flow velocity	0.5	m/s
Anode viscosity	$1.19\cdot10^{-5}$	Pa·s
Cathode viscosity	$2.46\cdot10^{-5}$	Pa·s
Hydrogen molar mass	0.002	kg/mol
Nitrogen molar mass	0.0028	kg/mol
Water molar mass	0.018	kg/mol
Oxygen molar mass	0.032	kg/mol
H_2-H_2O binary diffusion coefficient	$180.76\cdot10^{-6}$	m^2/s
N_2-H_2O binary diffusion coefficient	$5.0559\cdot10^{-5}$	m^2/s
O_2-N_2 binary diffusion coefficient	$4.7131\cdot10^{-5}$	m^2/s
O_2-H_2O binary diffusion coefficient	$5.5394\cdot10^{-5}$	m^2/s
Reference pressure	101000	Pa
Cell voltage	0.9	V
Anode exchange current density	1.105	$A\cdot m^{-2}$[11]
Cathode exchange current density	1	$A\cdot m^{-2}$[11]

2.3. Governing Equations

According to the aforementioned assumptions, the governing equations were presented as below.

Continuity and Momentum Conversation

The quntinuty equation is applied for fluid flow.

$$\nabla.(\rho u) = \sum S \tag{1}$$

Where S follows:

$$S = \sum \mathrm{R_i} \tag{2}$$

In the gas channels, equation (1) is equal to zero because chemical consumption or generation did not occur in the gas diffusion area.

The conversation of momentum is governed in the porous GDL using equations (3). And Navier-Stokes equation is used in the gas channel. And in the membrane, the velocity is equal to zero.

$$\frac{\mu}{\kappa} u = \nabla.\left(-PI + \frac{\mu}{\varepsilon}(\nabla u + (\nabla u)^T) - \left(\frac{2}{3}\mu\right)(\nabla u) I\right) \tag{3}$$

The gas density and molar mass are calculated from the ideal gas law formula as:

$$\rho = \frac{\mathrm{PM}}{\mathrm{RT}} \tag{4}$$

$$\mathrm{u} = -\frac{\kappa}{\mu}\nabla \mathrm{P} \tag{5}$$

Conservation of Species

A general form of Maxwell-Stefan equation is used to the transfer of multispecies gas in porous media.

$$\nabla \cdot \left[-\rho\omega_\mathrm{i} \sum_{\mathrm{j=1}}^{\mathrm{n}} \mathrm{D_{ij}^{eff}} \left\{\frac{\mathrm{M}}{\mathrm{M_j}}\left(\nabla\omega_\mathrm{j}\frac{\nabla \mathrm{M}}{\mathrm{M}}\right) + \left(\mathrm{x_j} - \omega_\mathrm{j}\right)\frac{\nabla \mathrm{P}}{\mathrm{P}}\right\} + \rho\omega_\mathrm{i}\mathrm{u}\right] = \mathrm{R_i} \tag{6}$$

$\mathrm{R_i}$ is a source term due to the reaction rate caused by oxidation and reduction on the cathode and anode respectively (kg.m^{-3} s^{-1}), where $\mathrm{D_{ij}^{eff}}$ is the effective diffusion coefficient:

$$\mathrm{D_{ij}^{eff}} = \mathrm{D_{ij}}.\varepsilon^{1.5} \tag{7}$$

On the cathode side, the transport equations are considered for two species as well as considering the following mass balance equation:

$$\omega_{\mathrm{N_2}} = 1 - \omega_{\mathrm{o_2}} - \omega_{\mathrm{H_2o}}\ ;\ \omega_{\mathrm{H_2o}} = 1 - \omega_{\mathrm{H_2}} \tag{8}$$

The reaction rate $\mathrm{R_i}$ corresponding to each species is given as:

$$\mathrm{R_{H_2}} = -\left(\frac{\mathrm{j_a}}{2\mathrm{F}}\right)\mathrm{M_{H_2}} \tag{9}$$

$$\mathrm{R_{O_2}} = -\left(\frac{\mathrm{j_c}}{4\mathrm{F}}\right)\mathrm{M_{o_2}} \tag{10}$$

$$\mathrm{R_{H_2o}} = -\left(\frac{\mathrm{j_c}}{4\mathrm{F}}\right)\mathrm{M_{H_2o}} \tag{11}$$

Conservation of Electric Charge

The current can be described as two parts: ionic current and electronic current. The ionic current is formed when protons transport through the membrane, while electrons pass through the electrodes to the external circuit (load), where an electronic current produces as result of these transfers. The electric charge equations are attained by Ohm's law as:

$$\mu\nabla.(-\sigma_\mathrm{s}\nabla.\phi_s) = \mathrm{S_s}\ ;\ \nabla.(-\sigma_\mathrm{m}\nabla.\phi_m) = \mathrm{S_m} \tag{12}$$

The source/sink terms in the electron and proton transport equations are caused by the existence of the electrochemical reaction, which takes place only in the reaction layers on electrodes, and they are formulated as:

Anode catalyst layer:

$$\mathrm{S_m} = \mathrm{j_a}\ ;\ \mathrm{S_s} = -\mathrm{j_a} \tag{13}$$

Cathode catalyst layer:

$$\mathrm{S_m} = \mathrm{j_c}\ ;\ \mathrm{S_s} = -\mathrm{j_c} \tag{14}$$

where, $\mathrm{j_a}$ and $\mathrm{j_c}$ are the transfer current density corresponding to the electrochemical reaction on the cathode and anode catalyst layers, respectively, which were calculated by employing Butler Volmer equation, and they are described by the following equation:

$$\mathrm{j} = \mathrm{ai_o^{ref}}\left(\frac{\mathrm{x_i P}}{\mathrm{P_{ref}}}\right)^{\gamma_\mathrm{i}}\left\{\exp\left[\frac{\alpha \mathrm{F}}{\mathrm{RT}}(\phi_\mathrm{s} - \phi_\mathrm{m})\right] - \exp\left[\frac{(1-\alpha)\mathrm{F}}{\mathrm{RT}}(\phi_\mathrm{s} - \phi_\mathrm{m})\right]\right\} \tag{15}$$

2.4. Boundary Conditions

This study considers the following boundary conditions:

- The current collector at the interface between the gas channel and GDL on the anode side is set to electric ground (0 V) and on the cathode side is set to cell operation potential.
- Velocity and temperature are defined at channel inlet.
- Channels outlet were subjected to the atmospheric pressure, and convective flux boundary conditions were applied.
- No slip boundary condition for all channel walls.

2.5. Numerical Methodology

COMSOL Multiphysics version 5.0 was used to solve the governing equations, mainly to calculate the

following unknown variables: velocity field vector u, pressure p, hydrogen mass fraction ω_{H_2}, oxygen mass fraction ω_{o_2}, water mass fraction ω_{H_2O}, electric potential ϕ_s and ionic potential ϕ_m. The computations were made on 64 bit Windows platform with 4 GB of RAM, and Inlet Core i5-2120 CPU 3.3 GHz processor. That was achieved by coupling two transports of concentrated species in porous media flow interface, under the section of chemical species transport physics, to one secondary current distribution interface under the section of electrochemistry physics. ϕ_s and ϕ_m in the electrodes, and ϕ_m in the membrane were obtained using the secondary current distribution interface through the modeling of electrochemical reactions.

3. RESULTS AND DISCUSSION

3.1. Model Validation

In this study, COMSOL was used to simulate HT-PEM fuel cell behavior under different operating conditions. The model can describe the investigation results of mass transport and electrical current distribution for the various HT-PEM fuel cell components, including the gas channels, gas diffusion layers, catalyst layers, membrane, and current collectors. The results were further calibrated and validated against previous experimental published results. Figure **2** shows a comparison of polarization curves obtained by the numerical simulation model and the previous published experimental data [24] at selected operating temperature and pressure of 150°C and 1atm, respectively. Gas channel dimensions, membrane properties and operating conditions used by Ubong *et al*. [24] were applied for this simulation. The simulated polarization curve showed a high agreement with the experimental result.

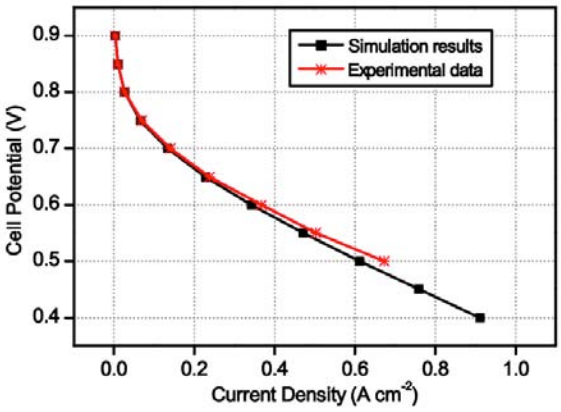

Figure 2: Comparison between experimental [9] and numerical polarization curves.

3.2. Oxygen Molar Concentration

Figure **3** shows the oxygen molar concentration at different subdomain boundaries within the cell. The molar concentration of oxygen is greater under the gas channel than under the current collector, and it is continuously consumed due to electrochemical reactions. Also, the oxygen molar concentration in the cathode electrode decreases along the flow direction from down to up, as shown in Figure **3**, and across the membrane. In addition, we can note that the highest molar concentration is 6.25 (mol/m^3) that appeared at T=120°C, which indicates that the rate of oxygen consumption along the flow direction is higher at T=180°C than at T=120°C mainly because of the increased chemical reaction rate in the cathode reaction layer at higher temperature.

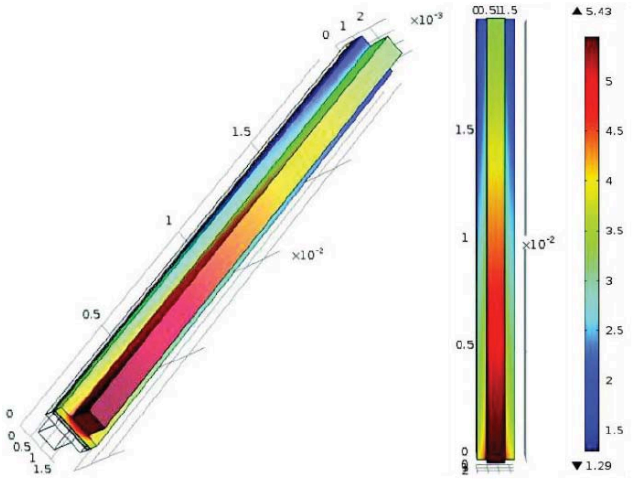

(a) T=180°C.

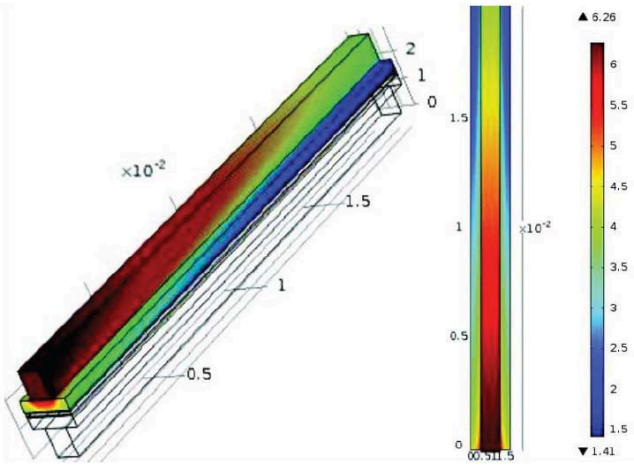

(b) T=120°C.

Figure 3: Oxygen molar concentration (mol m^{-3}) at V = 0.4 V for different operation temperature.

3.3. Hydrogen Molar Concentration

On the anode side, the hydrogen distribution profile is uniform, showing small gradients in x and z directions. It was expected that the hydrogen would easily reach electrochemical active site. It can be noted that the hydrogen concentration level is relatively even; we can observe clearly that the hydrogen concentration

slightly decreases as the anode gas flows through the channel from the inlet (at the bottom) to the outlet (at the top), see Figure **4**. This indicates that the resulting convective flux of anode gas headed for the membrane causes a small drop in the hydrogen concentration.

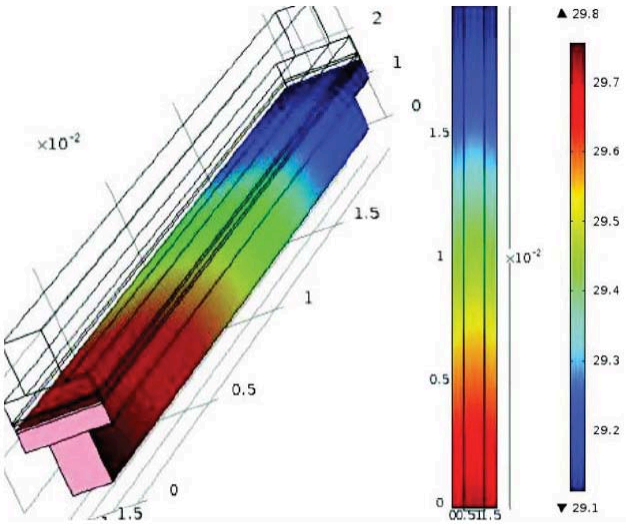

(a) T=120°C.

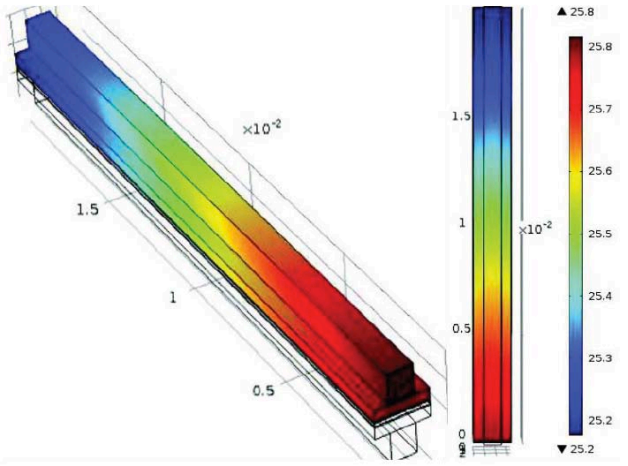

(b) T=180°C.

Figure 4: Hydrogen molar concentration (mol m^{-3}) at V = 0.4 V for different operation temperature.

3.4. Water's Vapor Concentration on both Electrodes Sides

Figure **5** shows the water vapor concentration in both anode and cathode sides. It is clear that water vapor is transported through diffusion and convection to the membrane. The concentration in the cathode side is greater as compared to the anode side due to the water production at the cathode. The results show a minimum concentration occurring near the inlet (at the top) on the anode side, see Figure **5a**, which reduces the fuel cell performance. Besides that, if the anode gas becomes too dry, the membrane will dry out, and that will decrease the ionic conductivity and damage the fuel cell. On the other hand, at the cathode side the water production increased along the fuel cell and the maximum water distribution level was found at the outlet (at the bottom), see Figure **5b**. Another critical condition could be observed if larger amount of water vapor accumulated in the lower corner of the membrane, basically because the water droplets might block the pores and badly affect the gas transport between the connected layers.

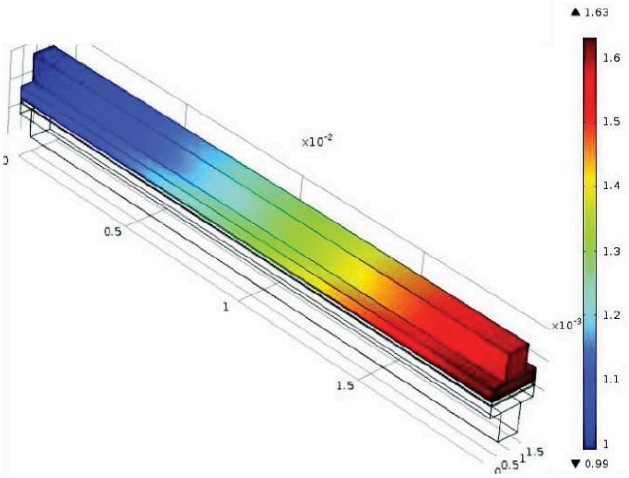

(a) Anode side

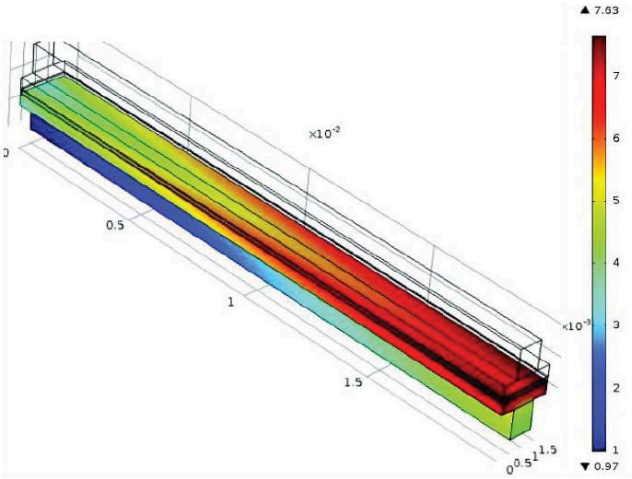

(b) Cathode side

Figure 5: Water's vapor concentration on anode and cathode sides at V = 0.4 V and T=120°C.

3.5. The Effect of Temperature in the HT-PEM Fuel Cell

Temperature variations have significant effects on the overall performance of the fuel cell, which recently led many researchers to study the thermal management of the fuel cell. Increasing the operating temperature not only improves the electrochemical reaction rate, but also enhances the mass transfer of

the reactants. However, rising the temperature may cause chemical degradation in the fuel cell, which declines the life time of the fuel cell. In order to investigate the effects of temperature change, the pressure remained constant at 1 atm while the temperature was varied from 120°C to 180°C. The polarization curves at various operating temperatures are presented. Figure **6** shows that an improved fuel cell performance can be obtained by rising the operating temperature. However, the gain is larger in the ohmic loss region than the activation over potential loss region, the performance is enhanced in all regions along the polarization curve. This observation could be clarified by the increase in reactants diffusivity and the enhanced membrane conductivity at higher temperatures.

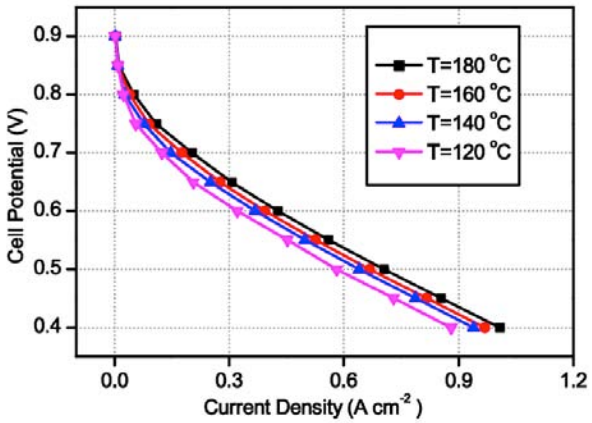

Figure 6: The effects of temperature on the performance of HT-PEM fuel cell at V = 0.4 V.

3.6. The Effect of Pressure on the HT-PEM Fuel Cell

The pressure is another operating parameter which has significant influence on fuel cell performance. In order to predict the effect of the pressure, the cell operating temperature was kept at 180°C, while the pressure was varied from 1 atm to 5 atm. Generally, running the cell under low operating pressures may result in reducing its current density and increasing the activation losses within the cell. Since the saturation pressure remains the same for constant operating temperature, the molar fraction of water vapor decreases with the increased total pressure. The polarization curves of different cell operating pressures are presented in Figure **7**. It was found that as the operating pressure increased from 1 atm to 5 atm, the fuel cell performance gradually improved. The performance progressively improved in the range of 1-3 atm, but the improvement declined as the pressure was increased above 3 atm. This increase in the fuel cell performance can be a new trend of the PEM fuel cell by developing HT-PEM fuel cell operating under higher pressure conditions.

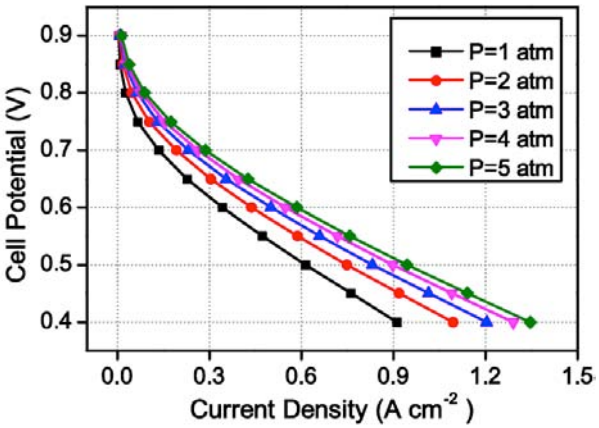

Figure 7: The effects of pressure on the performance of HT-PEM fuel cell at V = 0.4 V.

3.7. The Effect of GDL Porosity

The GDL has essential functions in the operation of PEM fuel cell, such as transporting the reactant gas supplied by flow channel to the CL, conducting the electrons with low resistance. The GDL is a very thin layer, composed of randomly oriented carbon fibers. In order to explore the effects of electrode porosity on fuel cell performance, Figure **8** presents the polarization curves for different GDL porosities, i.e., 0.2, 0.3, and 0.4. It is obvious that the fuel cell performs much better at higher GDL porosity because the porosity affects the amount of reactants mass transport from the channels to reaction layers hence higher porosity provides less resistance to mass transport. In contrast, increasing the GDL porosity has a negative effect on electron conduction because a higher porosity increases the electron transportation resistance through the gas diffusion layers.

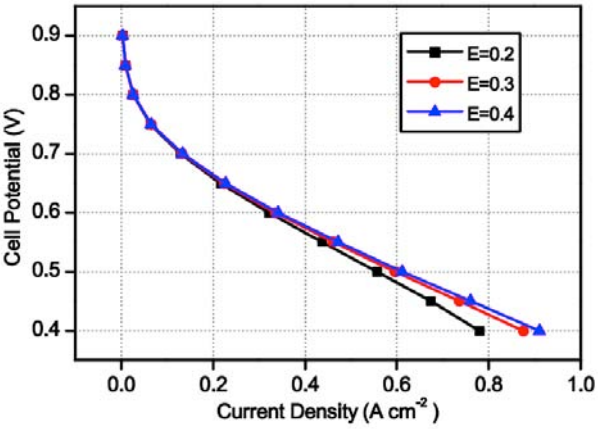

Figure 8: The effects of Porosity on the performance of HT-PEM fuel cell at V = 0.4 V.

3.8. GDL Permeability

Figures **9** and **10** show the variation of the current density of the fuel cell with the different GDL permeability under operating voltage equal to 0.4 V. Here, we aim to calculate the current density changes

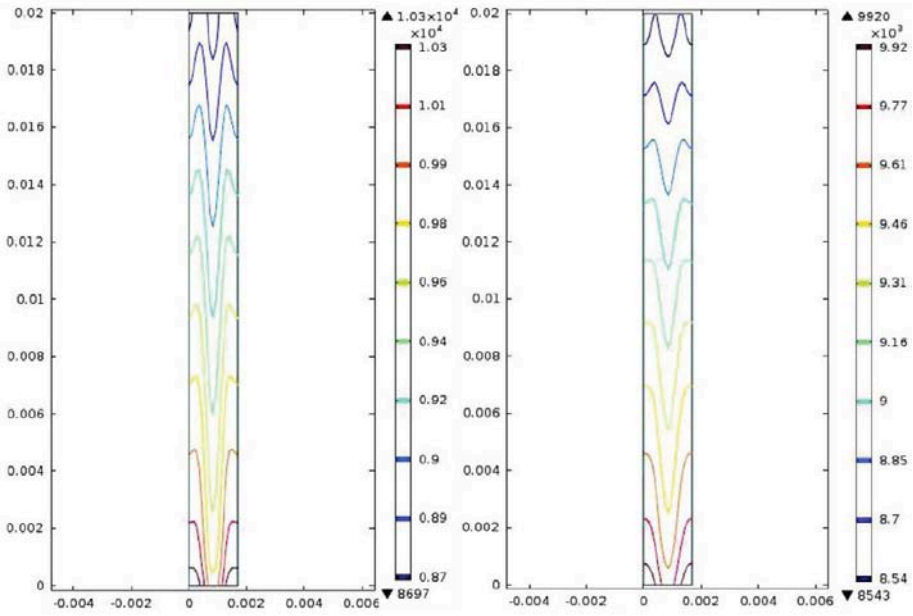

Figure 9: Current density variation with permeation rates of 1.18×10^{-9} m^2 (left) and 1.18×10^{-10} m^2 (right).

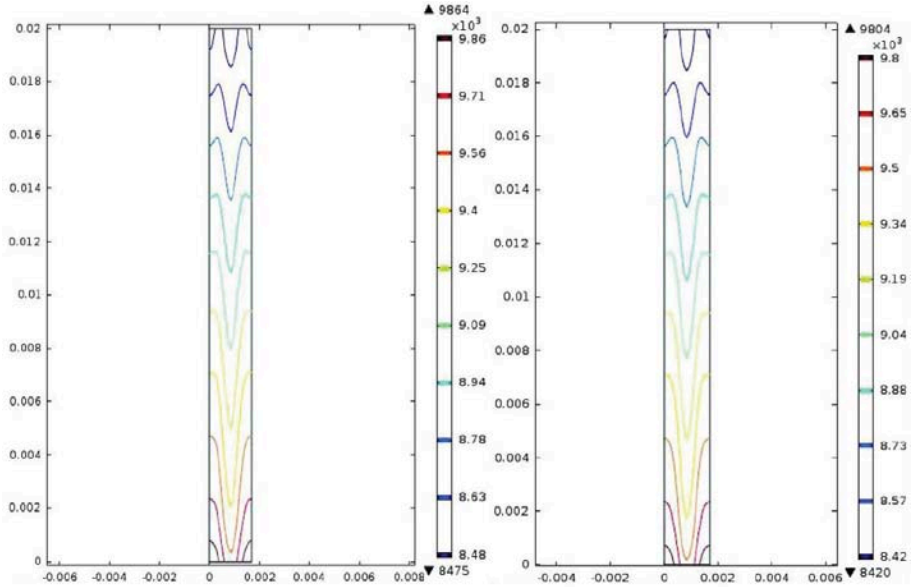

Figure 10: Current density variation with permeation rates of 1.18×10^{-11} m^2 (left) and 1.18×10^{-12} m^2 (right).

on the middle surface of the proton exchange membrane so that the horizontal and vertical coordinates represent the width and length of the proton exchange membrane, respectively. From Figures **9** and **10**, we can observe that as the GDL permeability increases from 1.18×10^{-12} m^2 to 1.18×10^{-9} m^2, the fuel cell current density gradually increases from 0.9804 A cm^{-2} to 1.07 A cm^{-2}, under the operating voltage of 0.4 volt. Therefore, it can be concluded that an improved output power density can be achieved by increasing the GDL permeability.

4. CONCLUSION

Three-dimensional HT-PEM fuel cell numerical model is performed using COMSOL to describe the behavior of the HT-PEM fuel cell. Good agreement between the simulation predictions and published experimental data has been obtained. Beside the detailed explanation about the transport phenomena inside the HT-PEM fuel cell, a parametric study was carried out to investigate the sensitivity of various operating and material parameters on HT-PEM fuel cell performance. The results from HT-PEM fuel cell modeling are presented and discussed in terms of reactants (hydrogen and oxygen) concentrations and water production on the anode and cathode sides; the polarization curves of the cell are also displayed. The performance of the fuel cell increases with the increasing temperature, as it could be expected. It is found that the performance improves when the pressure is increased. Also, the effects of increasing the porosity of the gas diffusion layer on the cell

performance were explored. The results show that the output power density can be improved by considering a gas diffusion layer characterized by a higher permeation rate. The presented model predictions can be further extended to identify the optimal operation and designs of HT-PEM fuel cell.

ACKNOWLEDGEMENTS

Financial support received from the Shanghai Automotive Industry Sci-Tech Development Foundation (No. 1706), the Guangdong Science and Technology Department (2015A030308019), and the Guangzhou Scientific and Technological Development Plan (201804020020) is gratefully acknowledged. One of the authors (AMD) is grateful to the financial support from the Chinese Scholarship Council (CSC) for Master student program and the University of Chinese Academy of Sciences (UCAS) scholarship for PhD student program.

NOMENCLATURE

A = effective surface area, m^2

D_{ij} = binary diffusivity, $m^2\ s^{-1}$

F = Faraday constant, $C\ mol^{-1}$

i = local current density, $A\ m^{-2}$

i_o = exchange current density, $A\ m^{-2}$

M = molecular mass, $kg\ mol^{-1}$

P = pressure, Pa

R = universal gas constant, $J\ mol^{-1}\ K^{-1}$

S = source/ sink terms

T = temperature, K

u = velocity vector, $m\ s^{-1}$

x = molar fraction

GREEK LETTERS

α = transfer coefficient

γ = concentration parameter

ε = porosity

φ = phase potential, V

σ = effective electric conductivity, $S\ m^{-1}$

ρ = gas mixture density, $kg\ m^{-3}$

ω = mass fraction

μ = dynamic viscosity, $kg\ m^{-1}\ s^{-1}$

κ = permeability, m^2

SUBSCRIPTS AND SUPERSCRIPTS

a = anode

c = cathode

eff = effective

e = electrolyte phase

i, j = species i, j

m = membrane

s = solid phase

REFERENCES

[1] Resitotlu IA, Altinisik K, Keskin A. The pollutant emissions from diesel-engine vehicles and exhaust aftertreatment systems. Clean Technol Environ Policy 2015; 17: 15-27. https://doi.org/10.1007/s10098-014-0793-9

[2] Shafiee S, Topal E. When will fossil fuel reserves be diminished ? Energy Policy 2009; 37: 181-9. https://doi.org/10.1016/j.enpol.2008.08.016

[3] Das V, Padmanaban S, Venkitusamy K. Recent advances and challenges of fuel cell based power system architectures and control - A review. Renew Sustain Energy Rev 2017; 73: 10-8. https://doi.org/10.1016/j.rser.2017.01.148

[4] O'hayre R, Cha SW, Colella W, Prinz FB. Fuel Cell Fundamentals. John Wiley & Sons 2016: 603. https://doi.org/10.1002/9781119191766

[5] Miller M, Bazylak A. A review of polymer electrolyte membrane fuel cell stack testing. J Power Sources 2011; 196: 601-13. https://doi.org/10.1016/j.jpowsour.2010.07.072

[6] Chippar P, Oh K, Kim D, Hong T, Kim W, Ju H. Coupled mechanical stress and multi-dimensional CFD analysis for high temperature proton exchange membrane fuel cells (HT-PEMFCs). Int J Hydrogen Energy 2012; 38: 7715-24. https://doi.org/10.1016/j.ijhydene.2012.07.122

[7] Authayanun S, Im-orb K, Arpornwichanop A. A review of the development of high temperature proton exchange membrane fuel cells. Chinese J Catal 2015; 36: 473-83. https://doi.org/10.1016/S1872-2067(14)60272-2

[8] Zhang C, Zhou W, Mousavi M, Wang Y, Hwa S. Determination of the optimal operating temperature range for high temperature PEM fuel cell considering its performance , CO tolerance and degradation. Energy Convers Manag 2015; 105: 433-41. https://doi.org/10.1016/j.enconman.2015.08.011

[9] Sousa T, Mamlouk M, Scott K. An isothermal model of a laboratory intermediate temperature fuel cell using PBI doped phosphoric acid membranes. Chem Eng Sci 2010; 10: 2513-30. https://doi.org/10.1016/j.ces.2009.12.038

[10] Xia L, Zhang C, Hu M, Jiang S. Investigation of parameter effects on the performance of high-temperature PEM fuel cell. Int J Hydrogen Energy 2018; 43: 23441-9. https://doi.org/10.1016/j.ijhydene.2018.10.210

[11] Araya SS, Zhou F, Liso V, Sahlin SL, Vang JR, Thomas S. A comprehensive review of PBI-based high temperature PEM fuel cells. Int J Hydrogen Energy 2016,41: 21310-44. https://doi.org/10.1016/j.ijhydene.2016.09.024

[12] Chandan A, Hattenberger M, El-kharouf A, Du S, Dhir A, Self V, *et al*. High temperature (HT) polymer electrolyte membrane fuel cells (PEMFC) A review. J Power Sources 2013; 231: 264-78. https://doi.org/10.1016/j.jpowsour.2012.11.126

[13] Rosli RE, Sulong AB, Daud WRW, Zulkifley MA. A review of high-temperature proton exchange membrane fuel cell (HT-PEMFC) system. Int J Hydrogen Energy 2017; 42: 9293-9314. https://doi.org/10.1016/j.ijhydene.2016.06.211

[14] Abdul Rasheed RK, Liao Q, Caizhi Z, Chan SH. A review on modelling of high temperature proton exchange membrane fuel cells (HT-PEMFCs). Int J Hydrogen Energy 2017; 42: 3142-65. https://doi.org/10.1016/j.ijhydene.2016.10.078

[15] Liu Y, Lehnert W, Janßen H, Can R. A review of high-temperature polymer electrolyte membrane fuel-cell (HT-PEMFC) -based auxiliary power units for diesel-powered road vehicles. J Power Sources 2016; 311: 91-102. https://doi.org/10.1016/j.jpowsour.2016.02.033

[16] Orfanidi A, Daletou MK, Neophytides SG. Applied Catalysis B : Environmental Preparation and characterization of Pt on modified multi-wall carbon nanotubes to be used as electrocatalysts for high temperature fuel cell applications. J Appl Catal B Environ 2011; 106: 379-89. https://doi.org/10.1016/j.apcatb.2011.05.043

[17] Kongstein OEÃ, Berning T, Børresen B, Seland F, Tunold R. Polymer electrolyte fuel cells based on phosphoric acid doped polybenzimidazole (PBI) membranes. Energy 2007; 32: 418-22. https://doi.org/10.1016/j.energy.2006.07.009

[18] Zhou F, Araya SS, Grigoras IF, Andreasen SJ, Kær SK. Performance Degradation Tests of Phosphoric Acid Doped Polybenzimidazole Membrane Based High Temperature Polymer Electrolyte Membrane Fuel Cells. J Fuel Cell Sci Technol 2014; 12: 1-9. https://doi.org/10.1115/FuelCell2014-6358

[19] Muthuraja P, Prakash S, Susaimanickam A, Manisankar P. Potential membranes derived from poly (aryl hexafluoro sulfone benzimidazole) and poly (aryl hexafluoro ethoxy benzimidazole) for high-temperature PEM fuel cells. Int J Hydrogen Energy 2018; 43: 21732-41. https://doi.org/10.1016/j.ijhydene.2018.03.058

[20] Cheddie D, Munroe N. Parametric model of an intermediate temperature PEMFC. J Power Sources 2006; 156: 414-23. https://doi.org/10.1016/j.jpowsour.2005.06.010

[21] Cheddie DF, Munroe NDH. A two-phase model of an intermediate temperature PEM fuel cell. Int J Hydrogen Energy 2007; 32: 832-41. https://doi.org/10.1016/j.ijhydene.2006.10.061

[22] Siegel C, Bandlamudi G, Heinzel A. Numerical Simulation of a High-Temperature PEM (HTPEM) Fuel Cell. Proc COMSOL Users Conf 2007: 1-7.

[23] Siegel C, Bandlamudi G, Heinzel A. Systematic characterization of a PBI/H3PO4 sol-gel membrane - Modeling and simulation. J Power Sources 2011; 196: 2735-49. https://doi.org/10.1016/j.jpowsour.2010.11.028

[24] Ubong EU, Shi Z, Wang X. Three-Dimensional Modeling and Experimental Study of a High Temperature PBI-Based PEM Fuel Cell. J Electrochem Soc 2009; 156: B1276- B1282. https://doi.org/10.1149/1.3203309

[25] Shamardina O, Chertovich A, Kulikovsky AA, Khokhlov AR. A simple model of a high temperature PEM fuel cell. Int J Hydrogen Energy 2010; 35: 9954-62. https://doi.org/10.1016/j.ijhydene.2009.11.012

[26] Peng J, Lee SJ. Numerical simulation of proton exchange membrane fuel cells at high operating temperature. J Power Sources 2006; 162: 1182-91. https://doi.org/10.1016/j.jpowsour.2006.08.001

[27] Reddy EH, Monder DS, Jayanti S. Parametric study of an external coolant system for a high temperature polymer electrolyte membrane fuel cell. Appl Therm Eng 2013; 58: 155-64. https://doi.org/10.1016/j.applthermaleng.2013.04.013

[28] Kvesić M, Reimer U, Froning D, Lüke L, Lehnert W, Stolten D. 3D modeling of a 200 cm^2 HT-PEFC short stack. Int J Hydrogen Energy 2012; 37: 2430-9. https://doi.org/10.1016/j.ijhydene.2011.10.055

[29] Lüke L, Janßen H, Kvesić M, Lehnert W, Stolten D. Performance analysis of HT-PEFC stacks. Int J Hydrogen Energy 2012; 37: 9171-81. https://doi.org/10.1016/j.ijhydene.2012.02.190

[30] Sousa T, Mamlouk M, Scott K. A Non-isothermal model of a Laboratory Intermediate Temperature Fuel Cell using PBI doped Phosphoric Acid Membranes. J Fuel Cells 2011; 44. https://doi.org/10.1002/fuce.200900178

[31] Jiao K, Zhou Y, Du Q, Yin Y, Yu S, Li X. Numerical simulations of carbon monoxide poisoning in high temperature proton exchange membrane fuel cells with various flow channel designs. Appl Energy 2013; 104: 21-41. https://doi.org/10.1016/j.apenergy.2012.10.059

[32] Salomov UR, Chiavazzo E, Fasano M, Asinari P. Pore- and macro-scale simulations of high temperature proton exchange fuel cells (HTPEMFC) and possible strategies for enhancing durability. Int J Hydrogen Energy 2017; 42: 26730-43. https://doi.org/10.1016/j.ijhydene.2017.09.011

[33] Ubeda D, Canizares P, Ferreira-Aparicio P, Antonio MC, Lobato J, Manuel AR. Life test of a high temperature PEM fuel cell prepared by electrospray. Int J Hydrogen Energy 2016; 41: 20294-304. https://doi.org/10.1016/j.ijhydene.2016.09.109

[34] Yang Y, Zhang X, Guo L, Liu H. Degradation mitigation effects of pressure swing in proton exchange membrane fuel cells with dead-ended anode. Int J Hydrogen Energy 2017; 42: 24435-47. https://doi.org/10.1016/j.ijhydene.2017.07.223

[35] Reimer U, Schumacher B, Lehnert W. Accelerated Degradation of High-Temperature Polymer Electrolyte Fuel Cells: Discussion and Empirical Modeling. J Electrochem Soc 2015; 162: F153-64. https://doi.org/10.1149/2.0961501jes

Received on 16-02-2020 Accepted on 22-03-2020 Published on 12-04-2020

DOI: http://dx.doi.org/10.15377/2409-5826.2020.07.1